

Research paper

Interlaboratory comparison of cosmogenic ^{21}Ne in quartz

Pieter Vermeesch^{a,b,*}, Greg Balco^c, Pierre-Henri Blard^e, Tibor J. Dunai^f, Florian Kober^a, Samuel Niedermann^g, David L. Shuster^{d,c}, Stefan Strasky^a, Finlay M. Stuart^h, Rainer Wieler^a, Laurent Zimmermann^e

^a Institute of Geochemistry and Petrology, ETH Zurich, Zürich, Switzerland

^b London Geochronology Centre, University College London, Gower Street, London WC1E 6BT, United Kingdom

^c Berkeley Geochronology Center, Berkeley, United States

^d Department of Earth and Planetary Science, University of California, Berkeley, United States

^e CRPG, UMR 7358, CNRS, Université de Lorraine, Vandoeuvre-lès-Nancy, F-54501, France

^f University of Cologne, Köln, Germany

^g Deutsches GeoForschungsZentrum GFZ, Potsdam, Germany

^h Scottish Universities Environmental Research Centre, Glasgow, United Kingdom

ARTICLE INFO

Article history:

Received 1 March 2012

Received in revised form

23 November 2012

Accepted 30 November 2012

Available online 10 December 2012

Keywords:

^{21}Ne

Quartz

Cosmogenic nuclides

Calibration

Standard

ABSTRACT

We performed an interlaboratory comparison study with the aim to determine the accuracy of cosmogenic ^{21}Ne measurements in quartz. CREU-1 is a natural quartz standard prepared from amalgamated vein clasts which were crushed, thoroughly mixed, and sieved into 125–250 μm and 250–500 μm size fractions. 50 aliquots of CREU-1 were analyzed by five laboratories employing six different noble gas mass spectrometers. The released gas contained a mixture of 16–30% atmospheric and 70–84% non-atmospheric (predominantly cosmogenic) ^{21}Ne , defining a linear array on the $^{22}\text{Ne}/^{20}\text{Ne}$ – $^{21}\text{Ne}/^{20}\text{Ne}$ three isotope diagram with a slope of 1.108 ± 0.014 . The internal reproducibility of the measurements is in good agreement with the formal analytical precision for all participating labs. The external reproducibility of the ^{21}Ne concentrations between labs, however, is significantly overdispersed with respect to the reported analytical precision. We report an average reference concentration for CREU-1 of $348 \pm 10 \times 10^6$ at $[\text{Ne}]/\text{g}[\text{SiO}_2]$, and suggest that the 7.1% (2σ) overdispersion of our measurements may be representative of the current accuracy of cosmogenic ^{21}Ne in quartz. CREU-1 was tied to CRONUS-A, which is a second reference material prepared from a sample of Antarctic sandstone. We propose a reference value of $320 \pm 11 \times 10^6$ at/g for CRONUS-A. The CREU-1 and CRONUS-A intercalibration materials may be used to improve the consistency of cosmogenic ^{21}Ne to the level of the analytical precision.

© 2012 Elsevier B.V. All rights reserved.

1. Introduction

Cosmogenic neon is a relatively little used tool for studying Earth surface processes. It is powerful for four reasons. First, it is produced and retained in quartz (Niedermann et al., 1993, 1994; Shuster and Farley, 2005) as well as most other silicates, such as pyroxene (Schäfer et al., 1999), olivine (Poreda and Cerling, 1992), sanidine (Kober et al., 2005), hornblende and biotite (Amidon and Farley, 2012). Therefore, it is applicable to most rock types found on the Earth's surface. Second, cosmogenic ^{21}Ne is a stable nuclide.

This gives it an age range limited essentially only by the erosion rate and allows exceptionally old landscapes to be dated (Schäfer et al., 1999; Dunai et al., 2005). Third, neon has three isotopes (^{20}Ne , ^{21}Ne , and ^{22}Ne), each of which have different abundances in the various reservoirs (atmospheric, nucleogenic, or magmatic) that may contribute to the natural ^{21}Ne background (Niedermann, 2002). By simultaneously analyzing all three isotopes and verifying whether they plot on a mixing line between atmospheric and spallogenic components, the cosmogenic neon method provides an internal 'reliability check' which is absent from other commonly used nuclides. Fourth, neon can be measured using a standard sector field noble gas mass spectrometer. Sample requirements are modest (typically 100–200 mg) and sample preparation is relatively straightforward as it does not require extensive chemical purification or chromatography. This greatly increases sample

* Corresponding author. London Geochronology Centre, University College London, Gower Street, London WC1E 6BT, United Kingdom.

E-mail address: p.vermeesch@ucl.ac.uk (P. Vermeesch).

throughput, which in turn opens up exciting opportunities for detrital work (Dunai et al., 2005; Codilean et al., 2008).

Cosmogenic ^{21}Ne is even more useful when combined with one or more cosmogenic radionuclides such as ^{10}Be or ^{26}Al . Such double- or triple-dating may be used for burial dating (Balco and Shuster, 2009a; Vermeesch et al., 2010), for catchment-wide erosion studies with complex exposure histories (Kober et al., 2009), or to measure the exposure age of old and very slowly eroding surfaces (Fujioka et al., 2005). An implicit assumption of many of these studies is that the accuracy of the ^{21}Ne method equals its analytical precision. Violation of this assumption may lead to erroneous results such as samples plotting in the 'forbidden zone' of the $^{21}\text{Ne}/^{10}\text{Be}$ two-nuclide diagram (Lal, 1991; Kober et al., 2011). An interlaboratory comparison study was set up in the framework of the CRONUS-EU initiative (Stuart and Dunai, 2009) with the aim to address this issue and provide the noble gas community with a well-characterized reference standard for the analysis of cosmogenic ^{21}Ne in quartz. The CREU-1 standard is a mixture of natural quartz pebbles, rich in cosmogenic ^{21}Ne , which were crushed and thoroughly homogenized to ensure optimal reproducibility (Section 2). Two size-fractions of CREU-1 were analyzed by five prominent cosmogenic noble gas laboratories, each of which used different experimental setups and data reduction protocols (Section 3). In total, 50 aliquots of CREU-1 were analyzed, with reported analytical precisions of 2–6%, but an external reproducibility of 7.1% (Section 4). These analyses were tied to a further 10 measurements of CRONUS-A, which is a second reference material prepared from an Antarctic quartzite analysed by two of the participating labs (Section 5).

2. Standard material

The CREU-1 standard material is pure quartz prepared from exposed vein-quartz clasts of a Miocene erosion surface ($19^{\circ}33'53.4''\text{S}$, $70^{\circ}7'1.5''\text{W}$, 930 m) in the Atacama desert near Pisagua, Chile (between sites B and C of Dunai et al., 2005). The clasts were shed onto the surface from local sources after the main sedimentation episode at ~ 12 – 14 Ma (Dunai et al., 2005). Approximately 400 g of material was mixed from five clasts (sample name CH04/5, pebbles 5, 6, 7, 8 and 13, weighing 81 g, 104 g, 77 g, 109 g and 55 g respectively) that had ^{21}Ne excess concentrations within 5% of their mean value. After crushing in a W-carbide disk mill, five size fractions were prepared using stainless steel sieves:

- 40–62 μm : 10.45 g, wet sieved and dried overnight at 50 $^{\circ}\text{C}$
- 63–125 μm : 40.62 g, wet sieved and dried overnight at 50 $^{\circ}\text{C}$
- 125–250 μm : 74.4 g, dry sieved
- 250–500 μm : 188 g, dry sieved
- >500 μm : 15.8 g, dry sieved

Of these five fractions, the 125–250 μm and 250–500 μm fractions were taken to produce the standard material, while the remaining fractions were preserved, but not processed any further. The 125–250 μm and 250–500 μm fractions were soaked in concentrated sulfuric acid at 120 $^{\circ}\text{C}$ overnight, to remove all iron coatings and accessory minerals such as rutile, sphene and fluorite. After the acid treatment, the material was rinsed ten times in cold de-ionized water, followed by five times 1 h ultrasonic rinsing in de-ionized water at 80 $^{\circ}\text{C}$. Next, the quartz was dried overnight at 110 $^{\circ}\text{C}$. Although the preparation steps outlined above probably already ensured a thoroughly mixed quartz sand, a FRITSCH[®] rotary cone sample divider laborette 27 was used to split the material into 16 equal fractions. Different aliquots of CREU-1 have been analyzed

by five noble gas laboratories, at BGC (Berkeley), CRPG (Nancy), ETH (Zürich), GFZ (Potsdam) and SUERC (Glasgow).

3. Analytical methods

The five participating laboratories employed a variety of noble gas mass spectrometers and analytical procedures for cosmogenic ^{21}Ne analysis. Rather than forcing all the participants to use the same heating schedules, getting times and so forth, they were allowed to use their own measurement routines, so that the calibration exercise fully captured the diversity of approaches used for ^{21}Ne analysis. The temperature steps and amount of material used are reported in Tables 1–3.

3.1. BGC

Neon extraction from quartz at BGC employed a 14-sample vacuum chamber with a 3 inch diameter sapphire viewport. Samples of up to 150 mg quartz were encapsulated in a Ta packet and heated through the viewport by a 150 W diode laser ($\lambda = 810$ nm) using a feedback control system in which the temperature of the packet was continuously monitored by an optical pyrometer coaxial with the laser delivery optic. Calibration of the pyrometer for the emissivity of the Ta packets was accomplished by placing a thermocouple in the same apparatus. Collateral heating of adjacent samples was prevented by completing one heating step for all samples before beginning the next heating step. This procedure was tested by interspersing blanks consisting of an empty Ta packet. After heating, sample gas was reacted with a SAES[®] getter and adsorbed to a cryogenic trap at 20 K. Neon was then released into the mass spectrometer at 70 K. All sample heating, gas processing, and measurement operations were automatically controlled. Analyses were done with a MAP-215 mass spectrometer updated with modern ion-counting electronics. Under normal operating conditions, this machine had a relatively low $\text{Ar}^+/\text{Ar}^{++}$ ratio (2.5–5, depending on source tuning) and inadequate mass resolution to fully resolve $^{20}\text{Ne}^+$ from $^{40}\text{Ar}^{++}$, so a correction for background $^{40}\text{Ar}^{++}$ was required. As described in Balco and Shuster (2009b), this was accomplished by introducing a ^{39}Ar spike and monitoring the Ar charge ratio as well as the $^{40}\text{Ar}^+$ signal throughout each analysis. The resulting correction on mass 20 varied between analyses, but was typically equivalent to $5.00 \pm 0.02 \times 10^8$ atoms ^{20}Ne . Similarly, a correction for $^{12}\text{C}^{16}\text{O}_2^{++}$ on mass 22 was made by establishing a relationship between the Ar and CO_2 charge ratios. Absolute calibration of Ne abundance was made by peak height comparison against an air standard processed in the same way as the samples and analyzed several times daily. Linearity of machine response was verified by varying the volume of the air standard. The pressure of the air standard reservoir was measured during loading with an MKS Baratron manometer, and corrected for atmospheric water vapor using three separate hygrometers at the time of air sample collection. Absolute volumes of the reservoir and pipette were determined by differential pressure measurements, again using the Baratron, against two separate reference glass ampules whose volumes were independently measured by Hg weighing. The amount of cosmogenic ^{21}Ne was calculated by assuming two-component mixing of atmospheric and cosmogenic neon. Reported uncertainties include i) counting uncertainties on all masses, including those used to generate corrections for $^{40}\text{Ar}^{++}$ and CO_2^{++} ; ii) uncertainty in blank subtraction (the ^{21}Ne process blank was ~ 0.5 Hz or $\sim 90,000$ atoms, which was $< 1\%$ of typical signals on mass 21 for these measurements); and iii) the reproducibility of the air standards ($\sim 1\%$ for ^{20}Ne , $\sim 3\%$ for ^{21}Ne).

Table 1
Summary table of the coarse fraction of CREU-1. '21/20' and '22/20' are the $^{21}\text{Ne}/^{20}\text{Ne}$ and $^{22}\text{Ne}/^{20}\text{Ne}$ ratios, $^{21}\text{Ne}^*$ is excess ^{21}Ne . Temperatures of ETH-4-7 (marked by an asterisk) and SUERC-8-9 (omitted) were set when the crucible was really full causing samples to be degassed at positions where the temperature was lower than the nominal crucible temperature. GFZ-6-7 were crushed to small grain size ($\sim 50\ \mu\text{m}$) before loading, while GFZ-8 was degassed by in vacuo crushing instead of heating. These samples were not included in Figs. 1 and 2.

	Mass [mg]	T [°C]	^{20}Ne [$\times 10^9$ at/g]	2 σ	21/20 [$\times 10^{-3}$]	2 σ	22/20 [$\times 10^{-3}$]	2 σ	$^{21}\text{Ne}^*$ [$\times 10^6$ at/g]	2 σ	Sum [$\times 10^6$ at/g]	2 σ
ETH-1	66.37	600	13.37	0.27	24.23	0.15	126.61	0.83	285.5	6.1	353.5	7.6
		800	9.85	0.20	6.96	0.11	105.59	0.67	39.6	1.0		
		1750	8.70	0.19	6.22	0.10	106.57	1.00	28.4	0.8		
ETH-2	66	600	11.45	0.24	27.78	0.26	129.17	0.74	285.1	6.5	348.5	7.7
		800	8.42	0.17	7.52	0.13	106.92	1.30	38.6	1.0		
		1750	6.62	0.18	6.70	0.14	105.90	0.98	24.9	0.8		
ETH-3	49.23	800	22.13	0.45	17.15	0.13	117.11	0.29	315.3	6.9	349.2	7.6
		1750	11.16	0.22	5.99	0.12	104.81	1.15	34.0	0.9		
ETH-4	82.13	600*	1.34	0.03	74.66	0.76	180.3	1.9	96.3	2.4	335.8	7.3
		800*	1.39	0.15	26.91	0.56	125.9	3.1	33.4	3.6		
		1750*	25.18	0.50	11.16	0.11	109.0	1.2	207.3	4.7		
ETH-5	48.56	600*	1.89	0.04	47.5	1.0	155.0	2.7	84.7	2.6	344.2	8.3
		800*	1.58	0.28	22.44	0.42	119.2	2.3	30.9	5.5		
		1750*	29.42	0.59	10.74	0.17	108.4	1.8	229.8	5.8		
ETH-6	48.73	600*	1.43	0.03	66.6	1.0	171.9	4.2	91.5	2.6	347.8	7.6
		800*	2.21	0.15	24.18	0.55	124.2	1.7	47.1	3.3		
		1750*	28.54	0.57	10.31	0.10	108.6	1.0	210.5	4.7		
ETH-7	81.3	600*	1.39	0.03	75.2	1.5	187.1	3.5	100.8	3.0	351.2	7.7
		800*	1.75	0.13	27.37	0.42	126.4	2.1	42.8	3.3		
		1750*	28.56	0.57	10.24	0.09	108.5	0.7	208.8	4.5		
BGC-1	109.9	370	4.1	1.5	24.4	9.1	117	49	86.9	6.0	368	12
		740	14.0	0.9	17.3	1.2	119	11	200.0	7.7		
		1140	20.3	1.3	7.0	0.5	105	8	81.5	7.4		
BGC-2	129.4	370	5.3	0.8	22.4	3.6	125	25	101.6	5.2	368	10
		740	15.0	0.5	15.9	0.6	114	7	194.9	7.4		
		1140	19.0	0.6	6.8	0.3	105	5	71.1	4.2		
BGC-3	115.7	390	4.7	0.6	28.2	3.6	132	32	121.3	6.9	378	15
		780	19.8	1.6	13.5	0.7	114	7	210	12		
		1140	12.7	0.5	6.7	0.4	109	6	46.5	4.1		
BGC-4	104.8	390	5.8	0.7	23.4	3.0	124	26	119.6	8.1	373	13
		780	16.5	0.9	15.4	0.9	113	8	203.4	8.6		
		1140	14.9	1.0	6.6	0.5	105	10	50.1	5.7		
BGC-5	103.5	370	3.1	0.6	32.3	6.0	137	67	90.7	6.9	374	14
		740	14.2	0.7	17.1	0.8	121	12	203.4	9.6		
		1140	22.7	1.2	6.5	0.3	108	5	79.6	7.5		
BGC-6	83.2	370	3.5	1.7	28	14	141	78	87.2	6.9	369	12
		740	12.9	0.8	18.3	1.2	122	11	201.9	7.8		
		1140	18.2	1.0	7.3	0.5	109	7	80.3	6.5		
BGC-7	75	390	6.3	2.0	17.8	5.7	115	43	92.4	8.6	353	17
		780	15.3	1.0	16.2	1.1	118	10	199	13		
		1140	17.6	0.9	6.6	0.4	110	8	61.8	6.1		
BGC-8	144.4	390	5.9	1.0	20.7	3.3	121	24	103.4	5.6	359	8
		780	15.3	0.5	16.0	0.6	115	5	196.3	4.4		
		1140	17.2	0.6	6.5	0.2	106	4	59.7	3.5		
BGC-9	110.2	370	3.9	0.6	28.9	4.8	139	42	101.7	5.8	369	13
		740	14.0	0.8	17.2	1.0	117	10	202	11		
		1140	18.9	0.6	6.6	0.3	108	5	65.5	5.3		
SUERC-1	165.1	1350	30.2	1.8	14.50	0.38	111.5	3.5	343	23	343	23
SUERC-2	239.6	480	1.82	0.11	24.12	0.80	127.8	5.8	37.9	2.7	301	10
		550	1.02	0.06	40.3	1.6	143.3	6.4	37.8	3.0		
		650	3.67	0.22	20.21	0.61	118.2	5.2	62.4	4.4		
		800	8.55	0.51	15.88	0.45	116.0	4.8	108.9	7.4		
		1400	18.0	1.1	6.02	0.14	105.2	3.9	54.2	3.5		
SUERC-3	258.4	480	4.91	0.29	25.10	0.67	125.4	5.5	107.3	7.2	380	12
		550	5.31	0.32	25.20	0.71	127.6	5.1	116.5	7.9		
		650	2.79	0.17	16.40	0.63	113.5	5.4	37.0	2.9		
		800	11.33	0.68	8.34	0.27	106.9	4.4	60.1	4.3		
		1200	14.73	0.88	6.20	0.17	104.7	4.4	47.0	3.2		
SUERC-4	203	1350	5.24	0.31	5.24	0.19	103.7	4.8	11.8	0.9	350	23
		1350	36.5	2.2	12.57	0.32	112.8	2.3	350	23		
		1350	33.8	2.0	13.32	0.30	114.4	2.3	349	23		
		1350	32.9	2.0	13.06	0.33	115.1	2.3	332	22		
		1350	40.6	2.4	11.59	0.23	110.8	1.6	350	23		
SUERC-8	237.3	–	17.7	1.1	19.33	0.33	119.5	1.5	289	18	317	18
		–	4.95	0.30	6.27	0.26	106.3	3.8	16.3	1.2		
		–	3.17	0.19	5.12	0.16	104.1	1.3	6.8	0.5		
		–	2.53	0.15	4.86	0.17	106.6	1.8	4.8	0.4		

Table 1 (continued)

	Mass [mg]	T [°C]	²⁰ Ne [×10 ⁹ at/g]	2σ	21/20 [×10 ⁻³]	2σ	22/20 [×10 ⁻³]	2σ	²¹ Ne* [×10 ⁶ at/g]	2σ	Sum [×10 ⁶ at/g]	2σ
SUERC-9	196.1	–	21.1	1.3	16.72	0.28	117.2	0.9	289	18		
		–	6.53	0.39	5.75	0.10	105.0	0.8	18.1	1.1		
		–	6.16	0.37	5.14	0.14	105.4	1.3	13.4	0.9		
SUERC-10	175.4	–	3.45	0.21	4.40	0.20	105.8	1.5	4.9	0.4	325	18
		1350	35.4	2.1	12.79	0.27	113.1	0.9	346	23		
		1350	0.81	0.05	2.60	0.85	105.8	3.8	–	–	346	23
SUERC-11	209.2	1350	11.88	0.71	25.00	0.44	126.3	1.1	260	16		
		1350	23.8	1.4	6.70	0.13	106.5	0.8	88.7	5.7	349	17
SUERC-12	187.8	1350	32.5	1.9	13.33	0.21	113.0	0.8	335	21		
		1350	0.88	0.05	4.45	0.43	105.5	3.4	1.3	0.2	336	21
SUERC-13	202.3	1350	33.5	2.0	13.59	0.22	114.5	0.8	355	22	355	22
SUERC-14	92.8	1350	39.7	2.4	12.22	0.12	111.5	0.5	357	22	357	22
GFZ-1	50.56	400	0.68	0.13	149	25	277	34	99.4	9.5		
		800	18.6	1.3	15.04	0.47	115.6	2.1	224	17		
		1200	5.65	0.47	6.70	0.41	107.4	4.5	21.2	2.6	345	20
GFZ-2	102.5	400	1.14	0.14	95.2	9.6	205	13	105.1	8.3		
		800	16.2	1.0	15.88	0.34	115.8	1.2	209	13		
		1200	11.34	0.73	6.32	0.12	105.9	1.4	38.1	2.6	352	16
GFZ-3	99.58	400	0.41	0.14	181	54	300	61	72.8	6.7		
		800	15.2	1.1	18.72	0.95	117.1	1.2	239	22		
GFZ-4	100.4	1200	11.75	0.84	6.33	0.19	103.4	1.2	39.6	3.5	351	23
		400	0.69	0.08	113	10	220	14	76.2	4.9		
GFZ-5	104.52	800	21.1	1.1	13.82	0.14	113.1	3.3	229	12		
		1200	10.79	0.58	6.22	0.20	104.5	0.8	35.2	2.9	340	13
GFZ-6	101.26	400	0.47	0.09	174	31	282	33	79.8	7.2		
		800	16.7	1.0	16.77	0.30	115.3	0.8	231	14		
		1200	9.42	0.56	6.42	0.18	107.5	1.3	32.5	2.5	343	16
GFZ-7	110.74	400	1.12	0.10	216	14	335	13	239	19		
		800	2.56	0.20	25.21	0.93	126.2	4.8	57.0	4.0		
GFZ-8	502.7	1200	0.05	0.06	4.2	4.4	90	35	0.1	0.2	296	19
		400	0.86	0.13	229	29	349	33	194	14		
GFZ-9	201.19	800	2.10	0.21	28.9	2.0	130.5	3.4	54.6	3.8		
		1200	0.00	0.10	–	–	–	–	0.1	0.2	249	15
GFZ-10	201.1	400	10.21	0.53	3.96	0.07	102.9	0.9	10.16	0.89	10.16	0.89
		600	1.05	0.11	97.7	5.9	207.3	7.2	99.1	7.5		
		800	3.74	0.28	32.69	0.61	133.7	2.7	111.2	8.1		
CRPG-1	149.1	800	12.66	0.92	10.00	0.16	110.3	0.7	89.2	6.7		
		1200	10.1	1.1	6.21	0.16	105.7	1.6	32.8	3.8	332	13
		400	2.37	0.19	57.3	3.1	162.8	3.4	129.2	7.3		
CRPG-2	83.3	600	5.45	0.32	24.60	0.69	126.5	1.4	118.2	6.7		
		800	10.34	0.61	7.79	0.15	106.6	0.6	50.0	3.2		
CRPG-1	149.1	1200	6.6	0.41	6.61	0.20	108.5	0.9	24.0	1.7	321	11
		820	14.15	0.54	21.7	1.2	122.4	6.5	267	19		
CRPG-2	83.3	1260	16.95	0.64	6.22	0.45	104.5	5.4	55.4	7.9	322	21
		1180	28.0	1.1	14.46	0.79	114.3	6.0	323	25		
		1260	0.03	0.16	12	79	–	–	0.3	2.6	323	26

3.2. CRPG

After 10 min cleaning in an acetone ultrasonic bath, quartz aliquots were wrapped in copper foils (Alfa Aesar[®], 0.025 mm thick, 99.8%). Samples were then loaded under high vacuum in a stainless steel carousel that had been baked during 10 h at 80 °C. Gas extraction from the quartz was realized by 25 min heating up to 1300 °C in a home-designed single vacuum resistance furnace with a boron nitride crucible (Zimmermann et al., 2012). Sequential purification with charcoals in liquid nitrogen, titanium sponges (Johnson-Matthey[®], mesh m3N8 t2N8) and SAES[®] getters (ST172/HI/20-10/650C) permitted gas cleaning by removal of H₂O, Ar, Kr, Xe and hydrocarbons. Ne was not separated from He. The purified gas was finally analyzed using a VG5400 mass spectrometer. Corrections for isobaric interferences of ⁴⁰Ar⁺⁺ at *m/e* = 20 and ¹²C¹⁶O₂⁺⁺ at *m/e* = 22 were negligible compared to the amount of analyzed neon. The mass spectrometer sensitivity was determined by peak height comparison against a 0.2 cm³ (~1.6 × 10¹⁰ atoms of ²⁰Ne) pipette of a gas standard having an atmospheric composition. Typical furnace blanks at 1000–1300 °C (25 min) were 1.0 ± 0.2 × 10⁸, 3 ± 1 × 10⁵ and 1.63 ± 0.06 × 10⁷ atoms of ²⁰Ne,

²¹Ne and ²²Ne, respectively. Excess ²¹Ne (²¹Ne*) concentrations were calculated following:

$$^{21}\text{Ne}^* = R_c \times ^{20}\text{Ne}_m \times (R_m - R_a) / (R_c - R_a) \quad (1)$$

where ²⁰Ne_m is the measured ²⁰Ne, *R_c* is the cosmogenic ²¹Ne/²⁰Ne-ratio (*R_c* = 0.8; Niedermann, 2002), *R_m* is the measured ²¹Ne/²⁰Ne-ratio, and *R_a* is the atmospheric ²¹Ne/²⁰Ne-ratio (*R_a* = 0.00296).

3.3. ETH

Noble gases were extracted by heating in a molybdenum crucible. Released gases were cleaned in a stainless steel extraction line equipped with Al/Zr-getters (SAES[®]) and activated charcoal held at the temperature of liquid nitrogen before He and Ne were expanded to a cryogenic pump. Helium and neon were separated by adsorbing neon at 14 K on stainless steel frits, pumping away the helium, and releasing the neon from the cryotrap at 50 K. Noble gas analyses were performed in a custom-made, all-metal magnetic sector mass-spectrometer (90°, 210 mm radius) equipped with a modified Baur-Signer ion source with essentially constant

Table 2
Same as Table 1, but for the fine fraction of CREU-1.

	Mass [mg]	T [°C]	²⁰ Ne [×10 ⁹ at/g]	2σ	21/20 [×10 ⁻³]	2σ	22/20 [×10 ⁻³]	2σ	²¹ Ne* [×10 ⁶ at/g]	2σ	Sum [×10 ⁶ at/g]	2σ
ETH-8	73.38	600	8.59	0.20	40.61	0.34	147.1	1.5	323.4	7.9	364	12
		800	6.78	0.21	6.21	0.18	107.6	1.3	22.1	0.9		
		1750	8.39	0.22	5.20	0.11	108.3	1.2	18.8	0.6		
ETH-9	70.42	600	9.91	0.21	35.20	0.31	142.6	1.1	319.3	7.4	356	11
		800	6.24	0.14	6.00	0.08	106.8	1.2	19.0	0.5		
		1750	8.11	0.16	5.13	0.15	105.7	1.5	17.7	0.6		
SUERC-15	378.6	450	3.17	0.19	58.9	1.5	164.5	5.3	174.6	11.4	345	13
		550	3.84	0.23	28.39	0.75	130.9	4.2	96.4	6.4		
		650	3.88	0.23	10.03	0.32	107.4	3.8	27.0	1.9		
		800	10.41	0.62	6.05	0.17	107.2	3.4	31.8	2.2		
		1350	9.36	0.56	4.62	0.16	104.2	3.3	15.3	1.1		
SUERC-16	237.1	550	0.86	0.05	52.0	1.9	158.5	8.8	41.8	3.2	359	13
		650	2.34	0.14	54.8	1.6	161.7	7.1	119.9	8.3		
		800	2.11	0.13	26.90	0.62	121.5	4.5	49.9	3.2		
		1350	24.5	1.5	8.85	0.20	108.0	4.0	142.2	9.1		
		480	0.73	0.04	10.14	0.81	106.4	5.6	5.2	0.6		
SUERC-17	33	1350	31.6	1.9	15.04	0.29	115.9	1.3	374.9	24.5	375	25
SUERC-18	156.2	1350	26.7	1.6	16.56	0.27	116.2	1.2	357.7	22.5	358	22
SUERC-19	166	1350	25.6	1.5	16.99	0.17	116.8	0.9	352.7	21.6	353	22
GFZ-11	100.24	400	0.96	0.13	152	16	263	18	143	14	330	17
		600	3.30	0.27	38.3	1.2	139.6	3.1	116.6	8.6		
		800	12.57	0.94	7.87	0.16	108.2	1.0	61.8	4.8		
		1200	3.33	0.30	5.66	0.34	104.3	4.1	9.0	1.2		

sensitivity over the pressure range relevant for this work (Baur, 1980). The ion source was equipped with a compressor device increasing the sensitivity by factors of 120 and 200 for ³He and ²¹Ne, respectively (Baur, 1999) compared to the sensitivities of the same spectrometer with the compressor turned off. The absolute sensitivity and mass discrimination of the mass spectrometer were determined by analysing known amounts of standard noble gas mixtures prepared from commercially available pure gases. The Ne isotopic composition of the standard gas was cross calibrated against two air standards (Heber et al., 2009). Similarly, the Ne

amounts delivered by the standard pipette were cross calibrated with air standards as well as with other independently filled standard gas bottles. The uncertainty of the Ne standard gas amounts is estimated to be 2% (Heber et al., 2009). Full procedural blanks (45' at 600°C + 20' at 800° + 15' at 1750 °C) were 1.211 ± 0.006 × 10⁸, 3.5 ± 0.2 × 10⁵, and 1.17 ± 0.01 × 10⁷ atoms of ²⁰Ne, ²¹Ne and ²²Ne, respectively. Corrections for isobaric interferences on mass 20 have been applied for ⁴⁰Ar⁺⁺ and H₂¹⁸O⁺ but were always less than 2%. No correction for CO₂⁺⁺ on ²²Ne was necessary. The low correction factors for doubly charged species were the

Table 3
Same as Tables 1 and 2, but for CRONUS-A.

	Mass [mg]	T [°C]	²⁰ Ne [×10 ⁹ at/g]	2σ	21/20 [×10 ⁻³]	2σ	22/20 [×10 ⁻³]	2σ	²¹ Ne* [×10 ⁶ at/g]	2σ	Sum [×10 ⁶ at/g]	2σ
BGC-10	137.7	390	2.21	0.72	69.28	22.43	172	59	144.4	8.2	338	14
		780	11.48	1.10	19.13	1.63	119	11	183.0	11.3		
		1140	1.65	0.35	9.53	2.16	110	36	10.6	1.8		
BGC-11	105.9	390	2.19	0.52	72.48	16.99	179	49	150.2	8.1	334	12
		780	9.72	0.77	21.06	1.67	126	12	173.2	8.4		
		1140	1.33	0.65	11.39	5.70	101	69	11.1	2.6		
BGC-12	122.5	370	2.68	1.24	50.59	23.39	140	72	124.7	6.5	337	8
		740	9.86	0.33	22.09	0.76	124	8	192.0	4.5		
		1140	2.11	0.63	12.35	3.72	122	43	20.0	2.5		
BGC-13	107.5	370	4.26	1.59	33.44	12.55	124	50	126.3	6.9	334	12
		740	11.27	1.11	20.37	2.07	118	15	195.1	7.7		
		1140	3.70	1.79	6.44	3.13	97	54	12.8	5.6		
BGC-14	66.7	370	4.18	0.89	32.74	7.03	138	46	123.7	5.5	336	11
		740	10.43	0.46	21.66	1.10	123	16	195.2	8.5		
		1140	2.13	0.89	11.16	4.81	128	77	17.2	3.6		
BGC-15	138.3	370	3.20	0.73	42.97	9.58	139	41	127.1	10.0	336	13
		740	10.24	0.42	22.06	0.68	123	8	193.1	8.7		
		1140	2.33	0.57	9.84	2.47	126	39	15.7	2.3		
BGC-16	167.8	390	4.53	0.63	33.39	4.36	135	21	138.3	8.1	352	13
		780	12.32	0.68	19.17	0.79	118	7	199.3	10.2		
		1140	1.93	0.52	10.52	2.91	122	46	14.0	2.1		
BGC-17	138.1	370	2.57	0.61	42.68	10.09	155	50	102.0	5.4	351	14
		740	11.97	0.64	21.61	0.99	123	9	226.3	12.9		
		1140	2.96	0.56	10.70	2.10	110	32	22.3	2.8		
BGC-18	144.8	370	2.47	0.39	42.38	6.57	153	56	97.0	8.0	341	11
		740	11.29	0.45	22.40	0.93	126	11	219.1	7.2		
		1140	3.93	0.50	9.24	1.26	114	26	24.8	2.7		
CRPG-3	37.2	1200	13.21	0.64	26.43	1.75	138	9	311.2	27.6	311	28
		1280	0.32	0.35	2.33	7.29	<DL	0	<DL	2.3		

results of a low electron acceleration voltage of 45 V in the ion source. Excess ^{21}Ne ($^{21}\text{Ne}^*$) concentrations were calculated with Equation (1).

3.4. GFZ

CREU-1 quartz samples were wrapped in aluminium foil and loaded in a sample carousel without further treatment, except for two aliquots of the 250–500 μm fraction (GFZ-6–7) which were crushed to $\sim 50 \mu\text{m}$ grain size in an agate mortar before loading. Noble gases were extracted in a resistance-heated furnace equipped with a tantalum crucible and molybdenum liner and analyzed in either of two VG5400 noble gas mass spectrometers, with measurements GFZ1–7 being measured on one machine, and GFZ8–11 on the other (Tables 1 and 2). GFZ-8 was not heated, but instead crushed in vacuo between two hard metal jaws in order to test whether Ne trapped in fluid inclusions of CREU-1 has an atmospheric isotopic composition. Gas purification involved a dry ice trap, two titanium sponge and foil getters, and two SAES[®] (Zr–Al) getters. The noble gases were trapped on stainless steel frits and/or activated charcoal in cryogenic adsorbers and sequentially released for He, Ne, and Ar–Kr–Xe analysis. Isobaric interferences of $^{40}\text{Ar}^{++}$ at $m/e = 20$ (up to 20% at 400 °C) and $^{12}\text{C}^{16}\text{O}_2^{++}$ at $m/e = 22$ (up to 10% at 400 °C) were corrected according to the method described by Niedermann et al. (1993, 1997). A correction for $\text{H}_2^{18}\text{O}^+$ at $m/e = 20$ was not necessary due to the mass resolution of ≥ 600 . Blanks had an atmospheric composition and contained $1\text{--}3 \times 10^7$ atoms of ^{20}Ne , depending on temperature. Excess ^{21}Ne was calculated without applying a blank correction, assuming an atmospheric origin of all the measured ^{20}Ne :

$$^{21}\text{Ne}^* = ^{21}\text{Ne}_m \times (R_m - R_a) / R_m \quad (2)$$

with all abbreviations as in Equation (1). In some cases a high atmospheric Ne memory (i.e., rapid decay of non-atmospheric Ne isotope ratios) required the application of a special procedure to derive the Ne concentration and isotopic composition at the time of gas admission to the mass spectrometer (see Goethals et al., 2009). Absolute noble gas concentrations were obtained by peak height comparison against a 0.1 cm^3 pipette of calibration gas (an artificial mixture of the five noble gases in nitrogen provided by Linde company; Niedermann et al., 1997), which was cross-calibrated in the 1990s against glass ampoule noble gas standards made available by O. Eugster (University of Bern) and whose noble gas concentrations are judged accurate to $\sim 3\%$ at 95% confidence level, and have been propagated into the overall uncertainty.

3.5. SUERC

The clean quartz was thoroughly rinsed in ultra-pure acetone and packed into aluminium foil cylinders. Cosmogenic Ne was extracted by heating each sample packet for 20 min. The active gases were removed by exposure to two hot SAES[®] (Zr–Al) getters during heating, and for a further 20 min as the furnace cooled. The heavy noble gases and residual active gases were subsequently adsorbed on liquid nitrogen cooled activated charcoal for 10 min and exposed to a getter at room temperature to adsorb hydrogen. Neon was then adsorbed on activated charcoal in a cryostatic cold head at 30 K. The helium was pumped for 1 min, then the Ne was desorbed from the charcoal trap at 100 K. Neon isotopes were analyzed statically in a MAP-215 magnetic sector mass spectrometer equipped with a modified Nier-type ion source, an axial electron multiplier (Burle Channeltron) operated in pulse-counting mode and a Faraday detector. A room temperature SAES[®] G50 getter and a liquid nitrogen-cooled activated charcoal trap were

used to minimize the contribution of interfering species during analysis. The data presented here were taken over a period of two years. Consequently source conditions changed to a small degree. Typically the source was tuned for Ne sensitivity prior to analytical periods; electron voltage of 88 V, trap current of 500 μA and an acceleration voltage of 3 kV. A slit in front of the electron multiplier was used to achieve a resolving power ($m/\Delta m$) of approximately 400. For all samples and calibrations the abundances of masses 18, 19, 20, 21, 22, 40 and 44 were determined by integrating counts recorded in 40–100 blocks of 5 s each. Peak heights of masses 2 and 16 were measured on the Faraday detector. Instrumental sensitivity was calculated from repeated analysis of aliquots of 2.2×10^{10} atoms ^{20}Ne in air sampled from a 5 L reservoir. Isotopic mass discrimination was approximately $0.50 \pm 0.03\%$ /amu. The average high temperature ^{20}Ne blank was 1×10^8 atoms. There was no observed increase when empty Al foil was heated. The Ne isotopic composition of blank measurements after correction for interfering species (see below) was indistinguishable from air ratios. Since it is likely that a significant amount of air-derived Ne is released from the quartz during heating, no blank correction has been made to the data. Excess ^{21}Ne concentrations were calculated assuming an atmospheric origin of all the measured ^{20}Ne according to Equation (2). Interference at $m/e = 20$ from $\text{H}_2^{18}\text{O}^+$ was calculated from measurement of $\text{H}_2^{16}\text{O}^+$ at mass 18. The contribution never exceeded 0.03%. No H^{19}F^+ signal was observed in blanks and mass spectrometer backgrounds. The dominant interference at $m/e = 20$ came from $^{40}\text{Ar}^{++}$. The charge state ratio $^{40}\text{Ar}^+ / ^{40}\text{Ar}^{++}$ is governed by the partial pressure of H in the mass spectrometer ionization region. A first-order relationship between $^{40}\text{Ar}^+ / ^{40}\text{Ar}^{++}$ and H⁺ beam size was recorded. The partial pressure of H remained constant resulting in $^{40}\text{Ar}^+ / ^{40}\text{Ar}^{++} = 2.30\text{--}2.32$. The contribution of $^{40}\text{Ar}^{++}$ to the measured ^{20}Ne signal in CREU quartz samples was $< 1\%$. Correction for $\text{C}^{16}\text{O}_2^{++}$ at $m/e = 22$ was calculated from measured mass 44 ($^{12}\text{C}^{16}\text{O}_2^{++}$) using a $\text{CO}_2^+ / \text{CO}_2^{++} = 50$ to 58 (determined by repeated measurements interspersed with sample measurements). No pressure dependence on the $\text{CO}_2^+ / \text{CO}_2^{++}$ ratio was recorded for a 50-fold variation in the partial pressure of H and CO_2 . Correction for interfering $^{12}\text{C}^{16}\text{O}_2^{++}$ never exceeded 1%.

4. Results

All five labs reported data for the coarse fraction, while three labs measured the fine fraction as well. The results for both sets of analyses are reported in Tables 1 and 2. The $^{21}\text{Ne}/^{20}\text{Ne}$ and $^{22}\text{Ne}/^{20}\text{Ne}$ compositions of the individual heating steps and their sums are consistent with a predominantly spallogenic origin of the released ^{21}Ne (Fig. 1). The pooled analyses comprise 16–30% atmospheric and 70–84% excess ^{21}Ne , with individual heating steps containing up to 98% excess ^{21}Ne . Linear regression of the spallation line yields a slope of 1.108 ± 0.014 (2σ), which is in statistical agreement with previously published values (Table 8 of Niedermann, 2002).

The total excess ^{21}Ne contents of all the aliquots are shown in Fig. 2. The reported 2σ analytical uncertainties are between 2 and 6%. The MSWD (Mean Square of the Weighted Deviates, a.k.a. ‘reduced Chi-square’, McIntyre et al., 1966) is reasonably close to unity for ETH, GFZ and BGC, indicating good agreement of the observed scatter with the measurement errors. The extremely low MSWD of 0.005 for CRPG may indicate overestimated analytical uncertainties, but could also be due to chance, as only two aliquots were analyzed. Finally, the coarse fraction of SUERC is characterized by an MSWD of 4.1, which may indicate underestimated analytical uncertainties. However, measurements of the fine fraction by the same lab have an MSWD of 1.3. There is no systematic difference between the fine and the coarse grain size fractions of ETH, SUERC

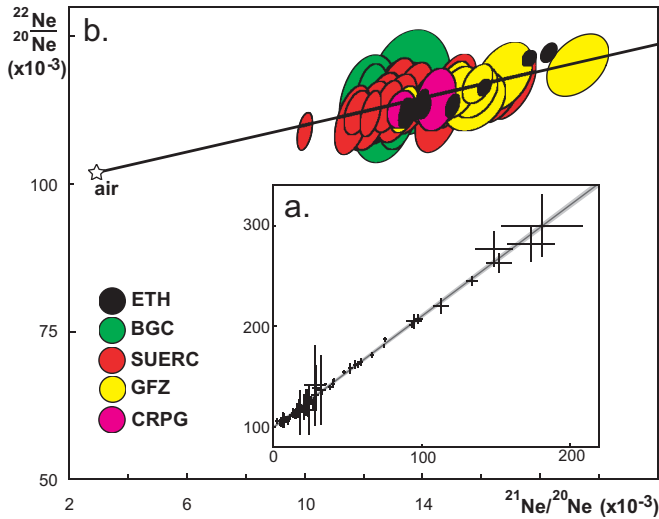


Fig. 1. Neon three-isotope plots of (a) all the individual heating steps and (b) the total released gas for each analyzed CREU-1 aliquot. The data fit a spallation line with a slope of 1.108 ± 0.014 (2σ , MSWD = 3.4). Error symbols are 1σ .

and GFZ. Measurements GFZ-6-7 were performed on material from the coarse fraction that was crushed for 5 min in air with an agate mortar to $\sim 50 \mu\text{m}$, resulting in some loss of excess ^{21}Ne . GFZ-8 was crushed in vacuo, and the data shown are for that crushing extraction. The ^{21}Ne excess of GFZ-8 is considerably less than the ^{21}Ne deficit in GFZ-6-7, probably because the in-vacuo crusher was much less efficient than the mortar. Measurements GFZ-6-8 were not included in subsequent calculations and figures. Total ^3He concentrations measured at GFZ were $204 \pm 10 \times 10^6$ at/g for the coarse fraction (seven measurements) and $109 \pm 7 \times 10^6$ at/g (a single analysis) for the fine fraction. The resulting ($^{21}\text{Ne}/\text{H}$) e-ratios are significantly greater than the production-rate ratio. This is likely caused by a combination of helium loss due to hot acid etching

during sample preparation, and the fact that helium is not quantitatively retained in quartz at surface temperatures (Shuster and Farley, 2005).

BGC analyzed material from two different vials of CREU-1, thus presenting an opportunity to verify the homogeneity of the standard. Measurements BGC-1-4 were performed on material from the same vial as ETH, whereas measurements BGC-5-8 were done on the same vial as CRPG. The observed difference between the two vials analyzed by BGC falls within the analytical uncertainty. The difference between the results of BGC and ETH/CRPG, however, falls well outside the statistically acceptable range. The error-weighted means of all the labs do not agree with each other within the analytical uncertainties, defined as the standard errors of those means. Therefore, in order to calculate a global average of all the data (using both the fine and the coarse grain fractions), we used a random effects model with two sources of uncertainty. We assume that the measurements x_i (where i is an identifier for each participating lab) come from a normal distribution of the form:

$$x_i \sim N(\mu, \sigma_i^2 + \zeta^2) \quad (3)$$

where μ is the global mean, σ_i^2 the analytical uncertainty (variance) of the i th lab, and ζ^2 is the amount of *overdispersion*, i.e. the excess scatter (variance) that cannot be explained by the analytical uncertainty alone. To understand this formula, consider the following two special cases. If $\sigma_i = 0$ (perfect reproducibility within each lab) then μ is the arithmetic mean of the laboratory averages. And if $\zeta = 0$ (perfect reproducibility between all labs) then μ is the error-weighted mean of those same laboratory averages. In order to simultaneously take into account the finite analytical precision of each lab and the variance between the labs, Equation (3) was iteratively solved for both μ and ζ , yielding an average ^{21}Ne concentration of $348 \pm 10 \times 10^6$ at/g and an *overdispersion* (defined as $2\zeta/\mu$) of 7.1%.

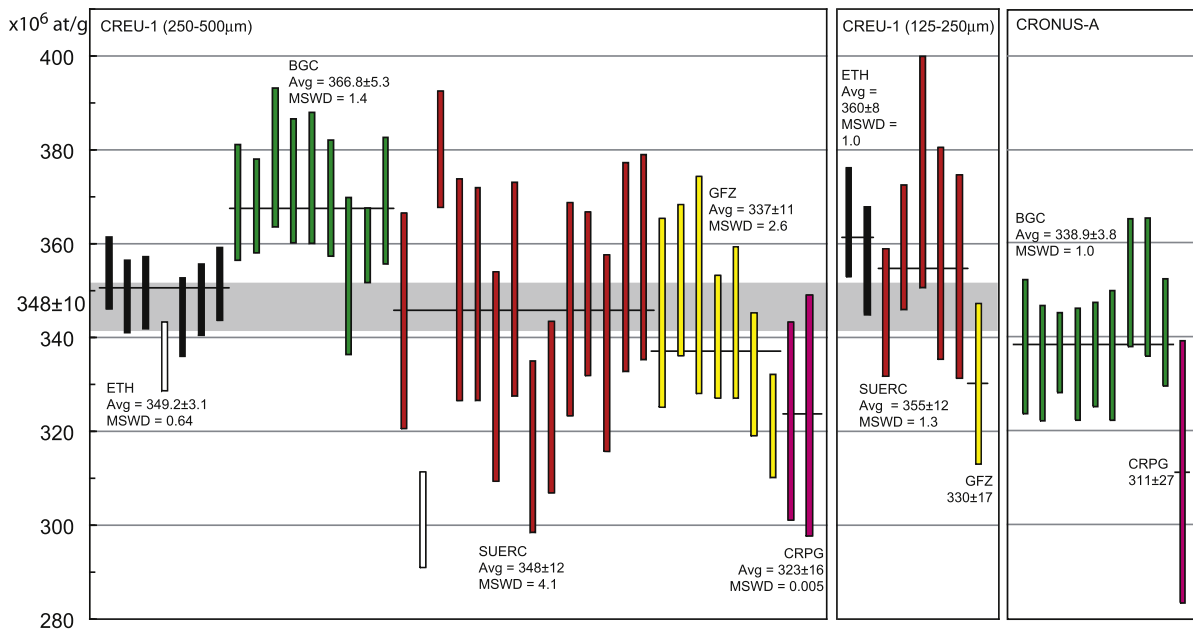


Fig. 2. Overview of all the reported ^{21}Ne concentrations and 2σ uncertainties, with indication of the error-weighted means for each participating laboratory. White bars are considered outliers and were not used to calculate the averages. Left and middle panels: coarse and fine fractions of CREU-1; right panel: CRONUS-A. Gray band marks the average and 2σ uncertainty of CREU-1.

5. Comparison with CRONUS-A

In addition to CREU-1, two of the participating labs also analyzed CRONUS-A as a second reference material. CRONUS-A was collected in Antarctica's Arena Valley (77°52'58.9"S, 160°56'35.1"E, 1666 m elevation), from a large (40 kg) yet thin (~2 cm) slab of Beacon sandstone. Quartz was purified at the University of Vermont by crushing, sieving and repeated etching in dilute HF, using procedures designed for cosmogenic ^{10}Be - ^{26}Al analysis. CRPG reported one and BGC a further nine analyses of CRONUS-A, using the same protocols that were used for the CREU-1 measurements (Table 3). The average cosmogenic ^{21}Ne content of the nine CRONUS-A samples measured by BGC was $338.9 \pm 3.8 \times 10^6$ at/g, i.e. $7.6 \pm 3.7\%$ lower than that of CREU-1. The single CRONUS-A analysis of CRPG is lower than its CREU-1 measurements by a similar amount ($4 \pm 17\%$), although the reported analytical precision of the latter estimate is much poorer. Additionally, published CRONUS-A values have been reported by two laboratories which did not participate in the interlaboratory comparison, at Harvard University ($330 \pm 3 \times 10^6$ at/g, Middleton et al., 2012) and the California Institute of Technology ($338 \pm 10 \times 10^6$ at/g, Amidon and Farley, 2012). Normalizing the average CRONUS-A value reported by BGC to the CREU-1 reference value results in a ^{21}Ne concentration of $320 \pm 11 \times 10^6$ at/g. We propose that when this value is used as a reference, CRONUS-A can serve as an alternative to CREU-1.

6. Discussion

It is interesting to note that significant amounts of excess ^{21}Ne remained trapped in the quartz after the second highest heating step, at temperatures of up to 820 °C. Total degassing was not achieved until the final temperature step at 1140 °C and more. This is significantly higher than the 800 °C release temperature for cosmogenic neon reported by Niedermann (2002). Nevertheless, for all samples of all labs, the data points of the higher temperature steps plot on the mixing line between atmospheric and cosmogenic neon (Fig. 1), which strongly suggests that the non-atmospheric neon in all samples is essentially purely cosmogenic, although quartz occasionally also contains a nucleogenic neon component released at high temperature with a $^{21}\text{Ne}/^{22}\text{Ne}$ ratio of approximately unity (Ne_{HT} , Niedermann et al., 1994; Niedermann, 2002). However, in view of the position of all data points in Fig. 1 it seems very improbable that a sizeable fraction of the non-atmospheric ^{21}Ne in our samples could be nucleogenic Ne_{HT} . Even in this unlikely case this would be largely irrelevant for the purpose of interlaboratory comparison, because for all samples we sum the non-atmospheric ^{21}Ne from all temperature steps.

Despite the fact that CREU-1 is pure and highly enriched in spallogenic neon, the ^{21}Ne concentrations reported by the participating labs are significantly overdispersed with respect to the formal analytical uncertainty. In theory, this overdispersion could be due to inhomogeneity of the standard material itself, as different labs analyzed aliquots from different vials of CREU-1. However, the analysis of two of these vials by BGC, and comparison with measurements of those same vials by ETH and CRPG, shows that this is not the case. Therefore, CREU-1 is homogenous. If the overdispersion cannot be attributed to the standard material itself, then it must be due to biases introduced by the different standard calibration bottles used (Heber et al., 2009), or to differences in the neon sensitivity between samples and standards introduced by sample processing or tuning conditions.

7. Conclusion

Our calibration experiment has shown that, although the reported analytical precision of cosmogenic noble gas measurements may be as low as 2%, the accuracy is not quite as good. We suggest that the 7.1% dispersion observed in our study be used as a more realistic estimate of the accuracy of the ^{21}Ne method at the present time. It should be borne in mind that this may even be an optimistic value, for a highly enriched and well behaved standard material. Using realistic and conservative analytical uncertainties is especially important for studies combining ^{21}Ne with other (radio) nuclides, and to assess the resolving power of such studies. For single nuclide studies, CREU-1 or CRONUS-A measurements can be used to normalize ^{21}Ne to the reference values reported in this paper, so that measurements from different labs can be compared on an equal footing and relative differences in ^{21}Ne can be compared on the level of the analytical precision (Dunai and Stuart, 2009). Those interested in obtaining aliquots of these standards may contact T. Dunai (tdunai@uni-koeln.de) for CREU-1 or T. Jull (jull@email.arizona.edu) for CRONUS-A.

Acknowledgments

This research was funded by CRONUS-EU (Marie Curie RTN project 511927). We would like to thank Mark Kurz and an anonymous reviewer for positive and constructive feedback on the submitted manuscript.

Editorial handling by: F.M Phillips

References

- Amidon, W.H., Farley, K.A., 2012. Cosmogenic ^3He and ^{21}Ne dating of biotite and hornblende. *Earth and Planetary Science Letters* 313–314 (0), 86–94.
- Balco, G., Shuster, D.L., 2009a. ^{26}Al - ^{10}Be - ^{21}Ne burial dating. *Earth and Planetary Science Letters* 286, 570–575.
- Balco, G., Shuster, D.L., 2009b. Production rate of cosmogenic ^{21}Ne in quartz estimated from ^{10}Be , ^{26}Al , and ^{21}Ne concentrations in slowly eroding Antarctic bedrock surfaces. *Earth and Planetary Science Letters* 281, 48–58.
- Baur, H., 1980. Numerische Simulation und praktische Erprobung einer rotations-symmetrischen Ionenquelle für Gasmassenspektrometer. Ph.D. thesis, ETH-Zürich No. 6596.
- Baur, H., 1999. A noble-gas mass spectrometer compressor source with two orders of magnitude improvement in sensitivity. *Eos, Transactions of the American Geophysical Union* 80, F1118.
- Codilean, A.T., Bishop, P., Stuart, F.M., Hoey, T.B., Fabel, D., Freeman, S.P.H.T., 2008. Single-grain cosmogenic ^{21}Ne concentrations in fluvial sediments reveal spatially variable erosion rates. *Geology* 36, 159–162.
- Dunai, T.J., González López, G.A., Juez-Larré, J., apr 2005. Oligocene Miocene age of aridity in the Atacama Desert revealed by exposure dating of erosion-sensitive landforms. *Geology* 33, 321–324.
- Dunai, T.J., Stuart, F.M., 2009. Reporting of cosmogenic nuclide data for exposure age and erosion rate determinations. *Quaternary Geochronology* 4 (6), 437–440.
- Fujioka, T., Chappell, J., Honda, M., Yatsevich, I., Fifield, K., Fabel, D., 2005. Global cooling initiated stony deserts in central Australia 2–4 Ma, dated by cosmogenic ^{21}Ne - ^{10}Be . *Geology* 33, 993.
- Goethals, M.M., Niedermann, S., Hetzel, R., Fenton, C.R., 2009. Determining the impact of faulting on the rate of erosion in a low-relief landscape: a case study using in situ produced ^{21}Ne on active normal faults in the Bishop Tuff, California. *Geomorphology* 103, 401–413.
- Heber, V.S., Wieler, R., Baur, H., Olinger, C., Friedmann, T.A., Burnett, D.S., 2009. Noble gas composition of the solar wind as collected by the Genesis mission. *Geochimica et Cosmochimica Acta* 73, 7414–7432.
- Kober, F., Alfimov, V., Ivy-Ochs, S., Kubik, P.W., Wieler, R., 2011. The cosmogenic ^{21}Ne production rate in quartz evaluated on a large set of existing ^{21}Ne - ^{10}Be data. *Earth and Planetary Science Letters* 302, 163–171.
- Kober, F., Ivy-Ochs, S., Leya, I., Baur, H., Magna, T., Wieler, R., Kubik, P.W., 2005. In situ cosmogenic ^{10}Be and ^{21}Ne in sanidine and in situ cosmogenic ^3He in Fe Ti-oxide minerals. *Earth and Planetary Science Letters* 236, 404–418.
- Kober, F., Ivy-Ochs, S., Zeilinger, G., Schlunegger, F., Kubik, P.W., Baur, H., Wieler, R., 2009. Complex multiple cosmogenic nuclide concentration and histories in the arid Rio Lluta catchment, northern Chile. *Earth Surface Processes and Landforms* 34 (3), 398–412.
- Lal, D., 1991. Cosmic ray labeling of erosion surfaces: in situ nuclide production rates and erosion models. *Earth and Planetary Science Letters* 104, 424–439.

- McIntyre, G.A., Brooks, C., Compston, W., Turek, A., 1966. The statistical assessment of Rb–Sr Isochrons. *Journal of Geophysical Research* 71, 5459–5468.
- Middleton, J., Ackert Jr., R., Mukhopadhyay, S., 2012. Pothole and channel system formation in the mcmurdo dry valleys of antarctica: new insights from cosmogenic nuclides. *Earth and Planetary Science Letters* 355–356, 341–350.
- Niedermann, S., 2002. Cosmic-ray-produced noble gases in terrestrial rocks: dating tools for surface processes. In: Porcelli, D., Ballentine, C.J., Wieler, R. (Eds.), *Noble Gases in Geochemistry and Cosmochemistry. Of Reviews in Mineralogy and Geochemistry*, vol. 47. Mineralogical Society of America, pp. 731–784.
- Niedermann, S., Bach, W., Erzinger, J., 1997. Noble gas evidence for a lower mantle component in MORBs from the southern East Pacific Rise: decoupling of helium and neon isotope systematics. *Geochimica et Cosmochimica Acta* 61, 2697–2715.
- Niedermann, S., Graf, T., Kim, J., Kohl, C., Marti, K., Nishiizumi, K., 1994. Cosmic-ray-produced ^{21}Ne in terrestrial quartz: the neon inventory of Sierra Nevada quartz separates. *Earth and Planetary Science Letters* 125 (1–4), 341–355.
- Niedermann, S., Graf, T., Marti, K., 1993. Mass spectrometric identification of cosmic-ray-produced neon in terrestrial rocks with multiple neon components. *Earth and Planetary Science Letters* 118, 65–73.
- Poreda, R.J., Cerling, T.E., 1992. Cosmogenic neon in recent lavas from the western United States. *Geophysical Research Letters* 19, 1863–1866.
- Schäfer, J.M., Ivy-Ochs, S., Wieler, R., Leya, I., Baur, H., Denton, G.H., Schlüchter, C., 1999. Cosmogenic noble gas studies in the oldest landscape on earth: surface exposure ages of the dry valleys, antarctica. *Earth and Planetary Science Letters* 167, 215–226.
- Shuster, D., Farley, K., 2005. Diffusion kinetics of proton-induced ^{21}Ne , ^3He , and ^4He in quartz. *Geochimica et Cosmochimica Acta* 69, 2349–2359.
- Stuart, F.M., Dunai, T.J., 2009. Advances in cosmogenic isotope research from CRONUS-EU. *Quaternary Geochronology* 4 (6), 435–436. Editorial.
- Vermeesch, P., Fenton, C.R., Kober, F., Wiggs, G.F.S., Bristow, C.S., Xu, S., 2010. Sand residence times of one million years in the Namib Sand Sea from cosmogenic nuclides. *Nature Geoscience* 3, 862–865.
- Zimmermann, L., Blard, P.-H., Burnard, P., Medynski, S., Pik, R., Puchol, N., 2012. A new single vacuum furnace design for cosmogenic ^3He dating. *Geostandards and Geoanalytical Research* 36, 121–129.